EIGHTEENTH EUROPEAN ROTORCRAFT FORUM

BU.06

Paper No. 68

SIMULTANEOUS TREATMENT OF FLEXION AND TORSION IN A GLOBAL MODAL APPROACH FOR THE CALCULATION OF BLADE DEFORMATIONS IN THE COMPREHENSIVE ROTOR CODE R85

by

Bernard BENOIT, *EUROCOPTER FRANCE*
Gilles ARNAUD, *EUROCOPTER FRANCE*

September 15-18, 1992

Avignon, FRANCE

ASSOCIATION AERONAUTIQUE ET ASTRONAUTIQUE DE FRANCE

SIMULTANEOUS TREATMENT OF FLEXION AND TORSION IN A GLOBAL MODAL APPROACH FOR THE CALCULATION OF BLADE DEFORMATIONS IN THE COMPREHENSIVE ROTOR CODE R85*

by

Bernard BENOIT, *EUROCOPTER FRANCE*
Gilles ARNAUD, *EUROCOPTER FRANCE*

ABSTRACT

In order to improve the prediction of rotor performance with the comprehensive rotor code R85 (1), special effort has been made to take torsion deformations of the blades into account.

In the soft blade version of R85, the blade deformation is approached by a modal summation ; each mode is described both by its components in flexion (lead-lag and flap) and in torsion.

This method is original in the sense that it does not artificially treat torsion on one side and flexion on the other, recombining them to get the overall deformation : torsion and flexion are fully coupled as far as modes are concerned.

In order to minimize the number of unknowns, the equations of motion are written in an energetic approach instead of a force-balance one :
Lagrange equations are solved and the blade deformation is obtained thereof. Since this way of resolution allows to account for both flexion and torsion behaviour of the blade, some reciprocal influence of flexion and torsion is included even if no coupling terms appear in the simplified elastic model used (Houbolt and Brooks (Ref 2)).

Validating calculations show a pretty good behaviour of the model. In this paper, comparisons with experiments will be thoroughly discussed. Effects of torsion to correlate the soft-in-torsion blade ROSOH experiments, with large tip deflexions, will be illustrated. Improvements obtained through the «PUMA RAE flight test workshop» (USA - GB - AUSTRALIA - FRANCE) by combining torsion and no-straight geometry in R85, mainly on local parameters (C_fM^2) and moments (flapping, torsion, lead-lag) will also be shown.

* *THIS WORK WAS SPONSORED BY DRET (FRANCE)*

1 INTRODUCTION

In order to improve the prediction of rotor performance with the comprehensive rotor code R85 (1) special effort has been made to take into account torsion deformations of the blades.

Up to now, torsion moment has been obtained by force integration, but torsion deformation was not taken into account in the calculations. However, since the torsion angle of an helicopter blade can be important (several degrees) and therefore not only creates torsion moment but also induces flapwise and chordwise bending moments, it must be included in an overall approach.

The method presented here is original in the sense that it does not treat torsion on one side and flexion on the other before recombining them to get the whole deformation :
torsion and flexion are fully coupled in the modes used to solve the energetic equations of rotor deformations.

After a brief presentation of the theoretical approach, comparisons between calculations, flight tests performed on the PUMA RAE and wind tunnel tests on ROSOH soft-in-torsion experimental rotor will be thoroughly discussed.

2 THEORETICAL APPROACH

2.1 Model for deformation

In the soft blade version of the R85 code, the deformation of the blade is described as the displacement of the reference axis of the blade (i. e., flexion deformation), followed by a rotation around the deformed axis (i. e., torsion deformation). Assuming that a section remains normal to the reference axis and that there is no extension of this axis, the deformation can be completely defined by three rotation angles (Figure 1). The first two ones ϕ_y (the local out-of-plane deformation angle) and ϕ_z the local in-plane deformation angle) give the total flexion deformation ; the third one θ_t is the local torsion angle.

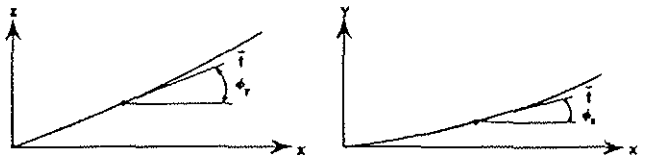

FIGURE 1 : FLEXION DEFORMATION OF THE REFERENCE AXIS OF THE BLADE

In practice, the reference axis is represented by a serie of rigid segments (Figure 2). At each rigid segment is associated :
- *a local flexion frame.*
- a rigid element of the blade that can rotate around the x_η-axis of the local reference frame.

The deformation in flexion is given by the rotation angles $\Delta\phi_{yI}$ and $\Delta\phi_{zI}$ of each segment in the reference frame of the preceding one.

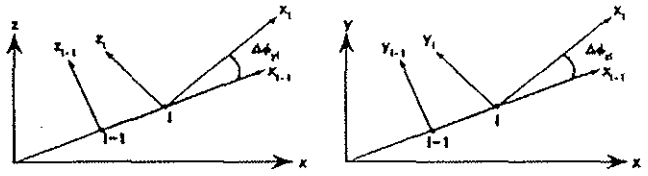

FIGURE 2 : MODELIZATION OF THE DEFORMATION OF THE REFERENCE AXIS OF THE BLADE

The torsion rotation is not applied to the reference frame, but only to the rigid elements of the blade associated with each segment. In this modelization, the torsion does not act on the reference axis. This allows the use of an elastic model without coupling terms between torsion and flexion.

2.2 Model for elasticity

The approach is derived from the one described by Houbolt and Brooks (2), valid for slender beams. The main assumption is the no-warping assumption :
each section remains normal to the elastic axis after deformation and the elastic axis is unvariant by any torsion rotation. The pitch axis of the blade, used as the reference axis, is often very close to the elastic axis. To simplify, they are supposed to be same. Assuming that there is no stretching along the span (i. e., no radial deformation), *the displacement of the elastic axis* under flexion can be expressed in function of the local out-of-plane and in-plane deformation angles, ϕ_y and ϕ_z. To link *strains and deformations*, the Hooke law is used (valid only for small linear elastic deformations of an isotropic material without creeping) :

$$\sigma_{rr} = E\gamma_{rr}$$

The resultant moments are then obtained, developping the *expression of the deformation* γ_{rr} *at any point of the section* for the first order in ϕ_y and ϕ_z, by integration of the strain field on the section.
This leads to :

$$M_y = E_{iB}(\phi'_y - \theta'\phi_z)$$

$$M_z = E_{iT}(\phi'_z + \theta'\phi_y)$$

Where $\theta = \theta_{vr} + \theta_e + \theta_t$

θ_{vr} : geometric twist
θ_e : *angle between geometric frame and elastic frame of the section*
θ_t : torsion angle

The torsion moment is expressed as :

$$Mx = G_j\theta'_t$$

In the expression of the moments, only the main terms have been kept, which completely decouples *torsion and flexion as* for as the elastic model is concerned.

Using the relation between the rotation angles ϕ_y and ϕ_z and the displacements of the reference axis, yields :

$$M_x = G_j\theta'_t$$

$$M_y = -E_{iB}(z''\cos\theta_L - y''\sin\theta_L)$$

$$M_z = E_{iT}(y''\sin\theta_L + z''\cos\theta_L)$$

With $\theta_L = \theta_{vr} + \theta_e$

2.3 Resolution

To describe the blade displacement with a low number of unknows, a modal summation is used ; each mode is described both by its components in flexion (lead-lag and flap) and in torsion.

The direction of the elastic axis under flexion is then computed step by step along the span.

The equations of motion are written in an energetic approach instead of a force-balance one.

Lagrange equations are solved and the blade deformation is obtained thereof :

$$\frac{d}{dt}\left(\frac{\partial T}{\partial \dot{q}}\right) - \frac{\partial T}{\partial q} + \frac{\partial U}{\partial q} = Q$$

T : kinetic energy
U : potential energy
Q : generalized force

In this method, no further approximation is made to compute *the kinetic energy and its derivatives*, and the inertial forces. All these terms are obtained through the real characteristics of each element of the blade, and the motion of the blade; no generalized characteristics of the blade are used.

In pratice, a low number of modes (less than 10) is enough to have a good approximation of blade deformations and stresses (see § 3).

As stated above, this method does not artificially treat torsion on one side and flexion on the other before recombining them *to get the overall deformation. Torsion and flexion* are fully coupled through the kinetic energy and aerodynamic forces calculation, despite the lack of coupling terms in the expression of the potential energy.

3 APPLICATION

3.1 Validation on the PUMA RAE workshop

A workshop involving the U.S.A., France, Great Britain and Australia gave the opportunity to all four nations to validate and compare their rotor codes for aeroelasticity to flight tests

performed on an AS 330 PUMA helicopter equipped with different tip blade shapes including the BERP style planform shape (Ref. 3) at RAE Bedford. The codes selected were CAMRAD run by Australia, CAMRAD/JA (U.S.A.), RAE/WHL (G.B.), and R85 (France).

At the time of the comparisons (1990), torsion moment was calculated by force integration in R85 while flatwise and edgewise bending moments were obtained from the modal curvatures method. In the following, torsion moments and deflections come from the modal curvatures method, developped above.

Moreover, to calculate the aerodynamic loads, the METAR vortex lattice method is coupled to a geometric blade curvature option in order to take into account swept tip effects.

Figure 3 shows comparisons on the oscillatory flatwise bending moment, at the advance ratio $\mu = 0.4$, between force integration and modal curvature methods. A typical 3/rev signal emerges from calculations. Their comparative results are pretty much the same, except for the inner part of the blade. It must be pointed out that the inner 10 % of the span have not been drawn on figures out in order to keep adequate comparative scales : indeed, the modal approach is unable to reproduce high concentrated variations of stresses such as those encountered when passing through the different rotor links, with a limited number of modes.

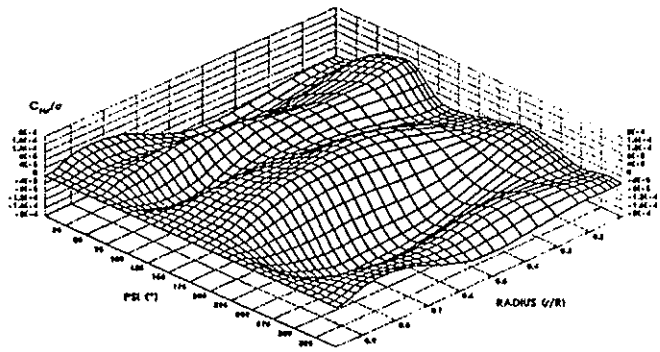

FIGURE 3a) : OSCILLATORY FLATWISE BENDING MOMENT COEFFICIENT : MODAL CURVATURES APPROACH

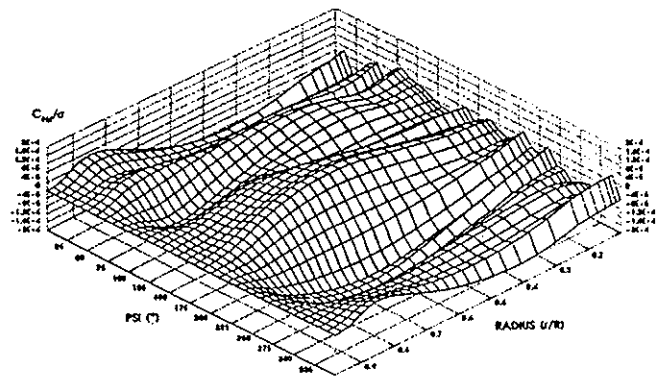

FIGURE 3b) : OSCILLATORY FLATWISE BENDING MOMENT COEFFICIENT : FORCE INTEGRATION APPROACH

In this calculation, 9 modes have been used : 5 flap ones, 3 lag ones and the first torsion one. All soft modes are fully coupled.

The example of the oscillatory flatwise bending moment near the last link illustrates quite well the limits of the modal approach : mathematically, five harmonic basic functions cannot approach an 8/rev (about) oscillatory function which besides, is obviously not C^{∞}(infinitely derivable). Therefore, the Lagrangian resolution, when converged thus, guarantees to get the same integral of the moment, either calculated from force integration or modal curvatures approach (energetic approach).

Such a behaviour of the modal approach would be found also when having concentrated masses leading to local discontinuities : the modal approach would smoothen the effects.

Figure 4 shows comparisons on the oscillatory edgewise bending moment at $\mu = 0.4$. Same comments as just above can be made for the inner part and the sharpest peak.

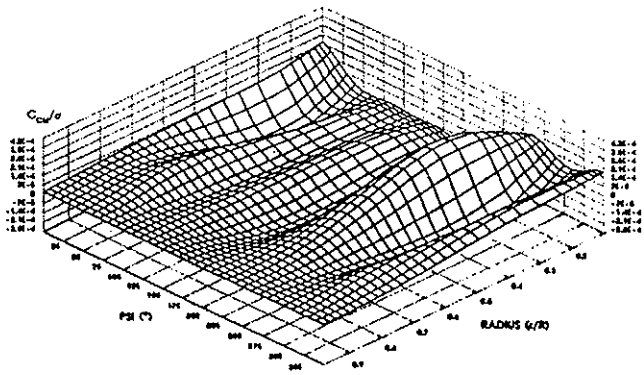

FIGURE 4a) : OSCILLATORY CHORDWISE BENDING MOMENT COEFFICIENT : MODAL CURVATURES APPROACH

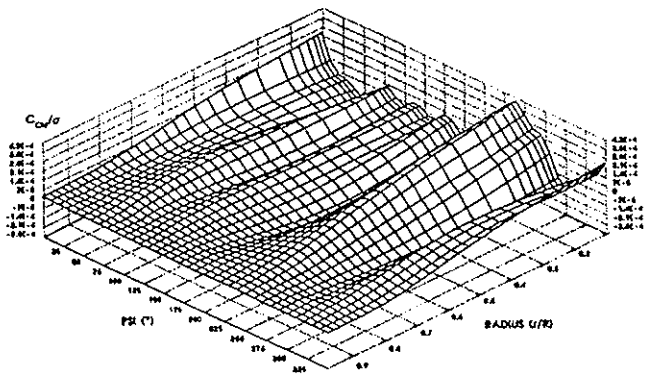

FIGURE 4b) : OSCILLATORY CHORDWISE BENDING MOMENT COEFFICIENT : FORCE INTEGRATION APPROACH

Figure 5 shows torsions comparisons : the convergence here between both calculations is remarkable, prooving the total coherence between the kinematic and the elastic models.

Figures 6, 7 and 8 show correlations between experiments and the different codes on 2D radial cross sections at 56.5 % R for the flatwise bending moment, 55 % R for the edgewise bending moment and the torsion moment.

All codes well predict the flatwise bending moment, though R85 and CAMRAD/JA have a weaker dynamic response in the retreating side (270° - 360°). For the chordwise bending moment, if R85 and CAMRAD/JA give the 4/rev signal measured during experiments, the phase for R85 is not accurate on the advancing side and none of the codes could predict the amplitude of the signal. This was attributed to a bad modelization of the dynamic characteristics of the hydraulic damper.

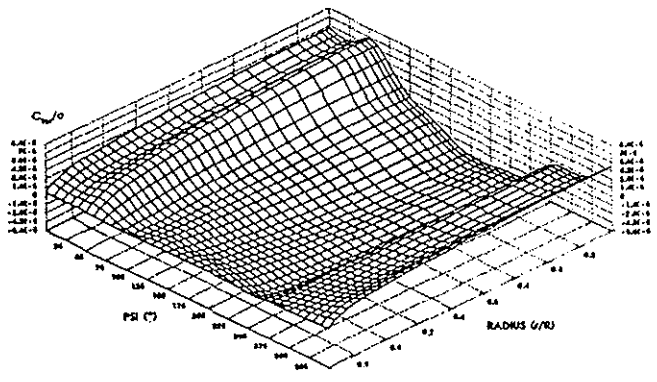

FIGURE 5a) : OSCILLATORY TORSION MOMENT COEFFICIENT : MODAL CURVATURES APPROACH

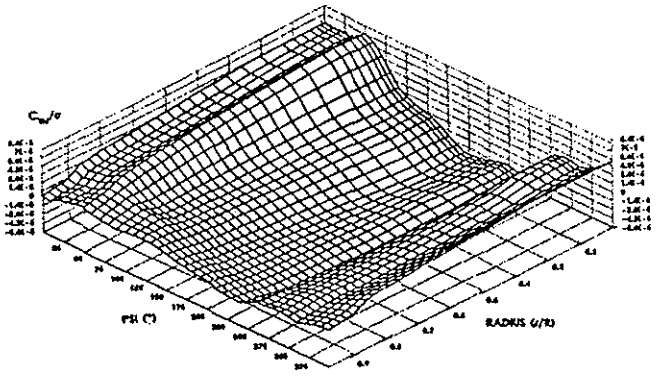

FIGURE 5b) : OSCILLATORY TORSION MOMENT COEFFICIENT : FORCE INTEGRATION APPROACH

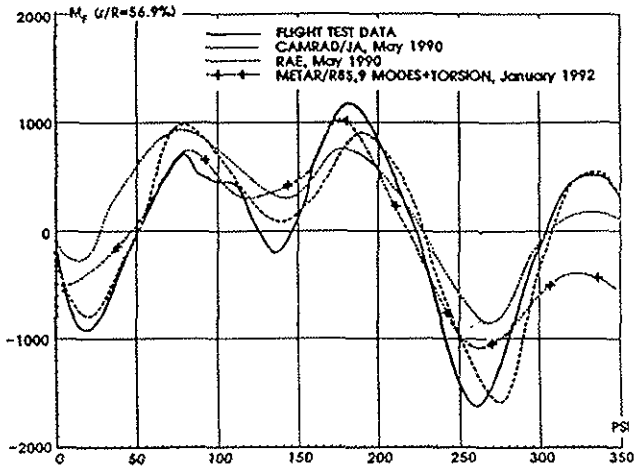

FIGURE 6 : FLATWISE BENDING MOMENT COMPARISONS AT r/R = 56.9 %

In the end, the torsion moment, though not well predicted by any code, shows a dominant one/rev excitation. The modifications brought to R85 (see above) led to this comparative prediction of the torsion moment obtained from the modal curvature approach. If the R85 signal is still poor in high harmonics, some excitation emerges anyway.
Because of the lack of dynamic response on the advancing side, the lift curve as a function of the azimut has been investigated.

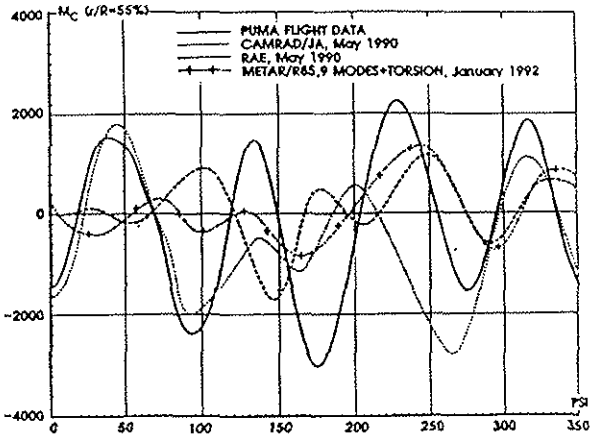

FIGURE 7 : CHARDWISE BENDING MOMENT COMPARISONS AT r/R = 55 %

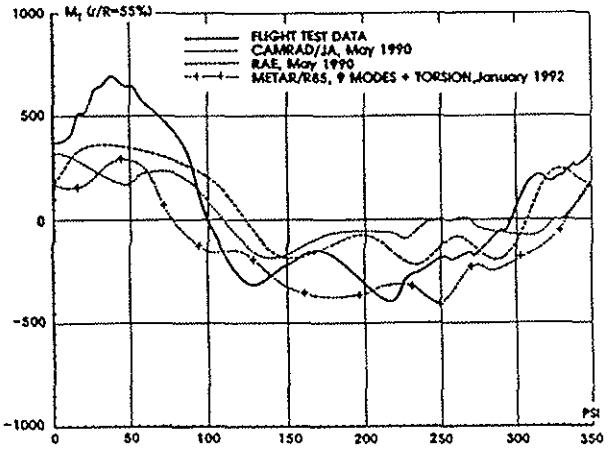

FIGURE 8 : TORSION MOMENT COMPARISONS AT r/R = 55 %

Figure 9 presents correlations on the lift ($C_z M^2$) in the outer part of the blade (r/R = 0.92 and r/R = 0.97) between R85 and the experiments, and shows improvements from a basic version of the code to a sophisticated one. The basic version is the following :

- external coupling between R85 and the induced velocities calculated by METAR.
- no torsion effects.
- no geometrical curvature effects.

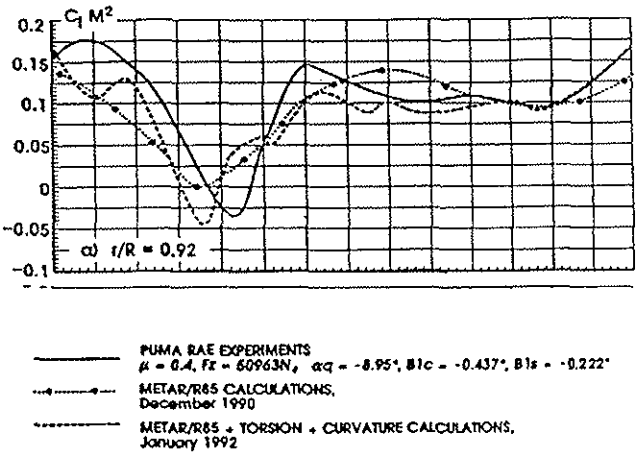

performed on an AS 330 PUMA helicopter equipped with different tip blade shapes including the BERP style planform shape (Ref. 3) at RAE Bedford. The codes selected were CAMRAD run by Australia, CAMRAD/JA (U.S.A.), RAE/WHL (G.B.), and R85 (France).

At the time of the comparisons (1990), torsion moment was calculated by force integration in R85 while flatwise and edgewise bending moments were obtained from the modal curvatures method. In the following, torsion moments and deflections come from the modal curvatures method, developped above.

Moreover, to calculate the aerodynamic loads, the METAR vortex lattice method is coupled to a geometric blade curvature option in order to take into account swept tip effects.

Figure 3 shows comparisons on the oscillatory flatwise bending moment, at the advance ratio $\mu = 0.4$, between force integration and modal curvature methods. A typical 3/rev signal emerges from calculations. Their comparative results are pretty much the same, except for the inner part of the blade. It must be pointed out that the inner 10 % of the span have not been drawn on figures out in order to keep adequate comparative scales : indeed, the modal approach is unable to reproduce high concentrated variations of stresses such as those encountered when passing through the different rotor links, with a limited number of modes.

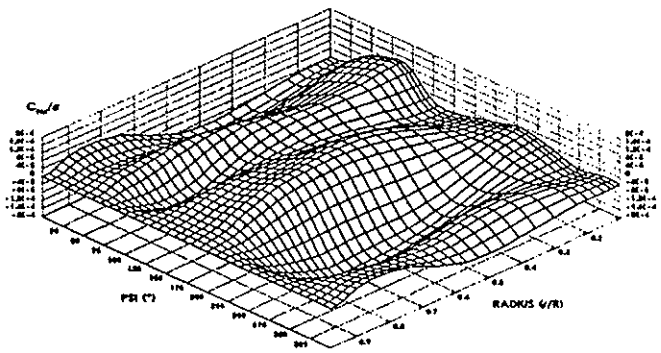

FIGURE 3a) : OSCILLATORY FLATWISE BENDING MOMENT COEFFICIENT : MODAL CURVATURES APPROACH

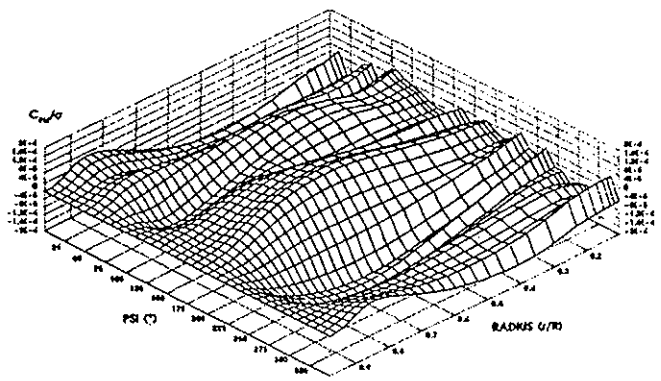

FIGURE 3b) : OSCILLATORY FLATWISE BENDING MOMENT COEFFICIENT : FORCE INTEGRATION APPROACH

In this calculation, 9 modes have been used : 5 flap ones, 3 lag ones and the first torsion one. All soft modes are fully coupled.

The example of the oscillatory flatwise bending moment near the last link illustrates quite well the limits of the modal approach : mathematically, five harmonic basic functions cannot approach an 8/rev (about) oscillatory function which besides, is obviously not C^{∞}(infinitely derivable). Therefore, the Lagrangian resolution, when converged thus, guarantees to get the same integral of the moment, either calculated from force integration or modal curvatures approach (energetic approach).

Such a behaviour of the modal approach would be found also when having concentrated masses leading to local discontinuities : the modal approach would smoothen the effects.

Figure 4 shows comparisons on the oscillatory edgewise bending moment at $\mu = 0.4$. Same comments as just above can be made for the inner part and the sharpest peak.

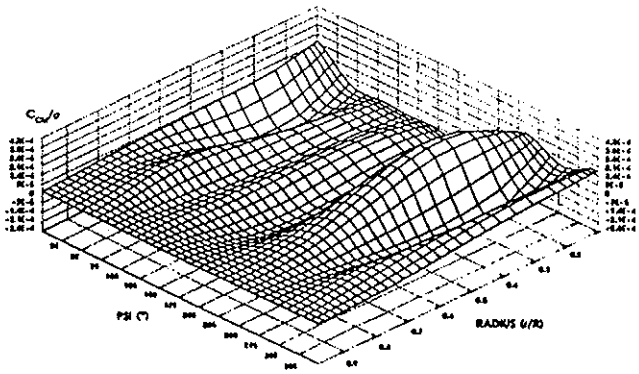

FIGURE 4a) : OSCILLATORY CHORDWISE BENDING MOMENT COEFFICIENT : MODAL CURVATURES APPROACH

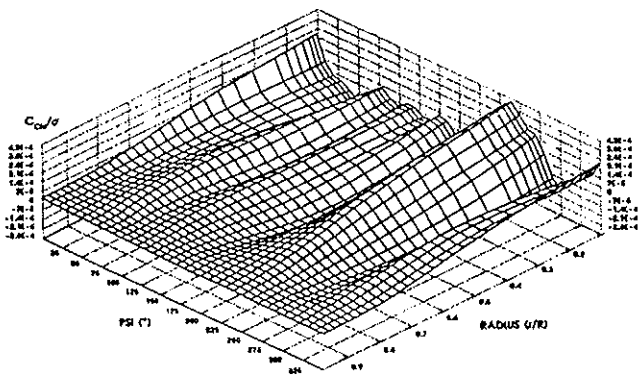

FIGURE 4b) : OSCILLATORY CHORDWISE BENDING MOMENT COEFFICIENT : FORCE INTEGRATION APPROACH

Figure 5 shows torsions comparisons : the convergence here between both calculations is remarkable, prooving the total coherence between the kinematic and the elastic models.

Figures 6, 7 and 8 show correlations between experiments and the different codes on 2D radial cross sections at 56.5 % R for the flatwise bending moment, 55 % R for the edgewise bending moment and the torsion moment.

All codes well predict the flatwise bending moment, though R85 and CAMRAD/JA have a weaker dynamic response in the retreating side (270° - 360°). For the chordwise bending moment, if R85 and CAMRAD/JA give the 4/rev signal measured during experiments, the phase for R85 is not accurate on the advancing side and none of the codes could predict the amplitude of the signal. This was attributed to a bad modelization of the dynamic characteristics of the hydraulic damper.

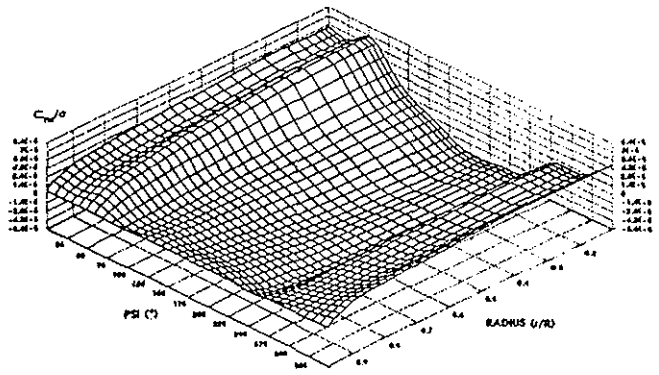

FIGURE 5a) : OSCILLATORY TORSION MOMENT COEFFICIENT : MODAL CURVATURES APPROACH

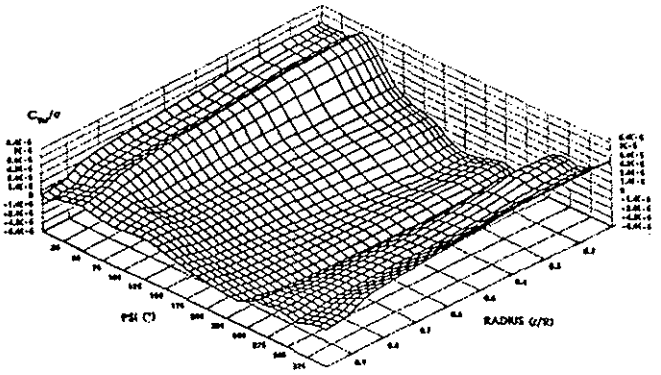

FIGURE 5b) : OSCILLATORY TORSION MOMENT COEFFICIENT : FORCE INTEGRATION APPROACH

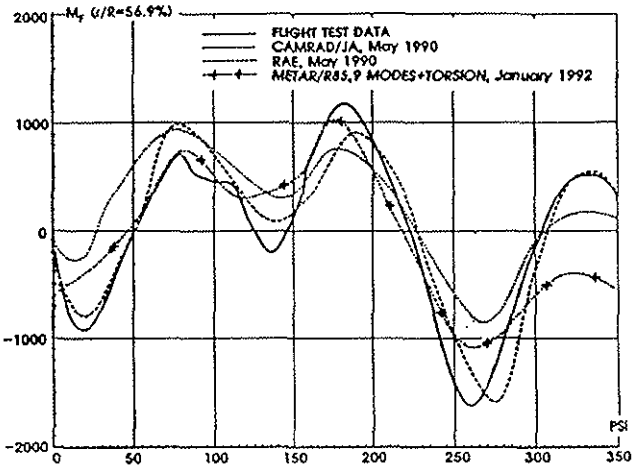

FIGURE 6 : FLATWISE BENDING MOMENT COMPARISONS AT r/R = 56.9 %

In the end, the torsion moment, though not well predicted by any code, shows a dominant one/rev excitation. The modifications brought to R85 (see above) led to this comparative prediction of the torsion moment obtained from the modal curvature approach. If the R85 signal is still poor in high harmonics, some excitation emerges anyway.
Because of the lack of dynamic response on the advancing side, the lift curve as a function of the azimut has been investigated.

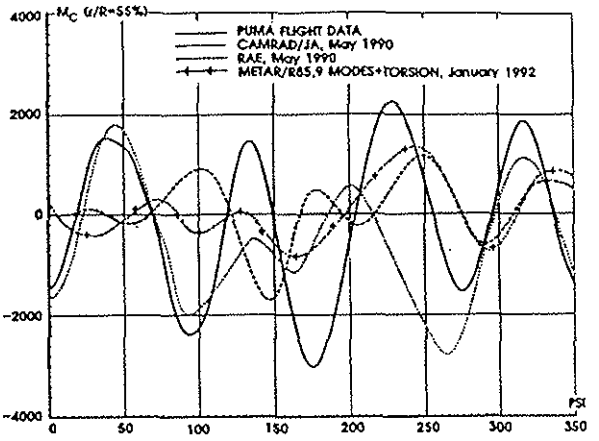

FIGURE 7 : CHARDWISE BENDING MOMENT COMPARISONS AT r/R = 55 %

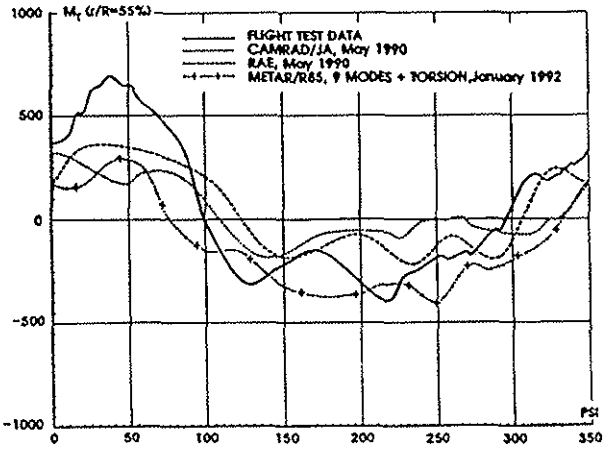

FIGURE 8 : TORSION MOMENT COMPARISONS AT r/R = 55 %

Figure 9 presents correlations on the lift ($C_z M^2$) in the outer part of the blade (r/R = 0.92 and r/R = 0.97) between R85 and the experiments, and shows improvements from a basic version of the code to a sophisticated one. The basic version is the following :

- external coupling between R85 and the induced velocities calculated by METAR.
- no torsion effects.
- no geometrical curvature effects.

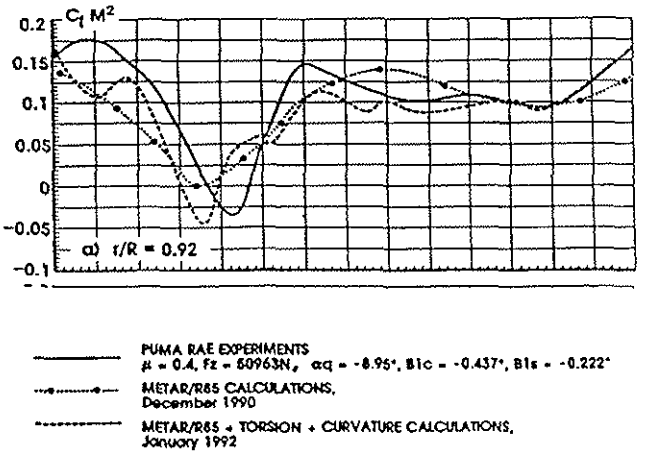

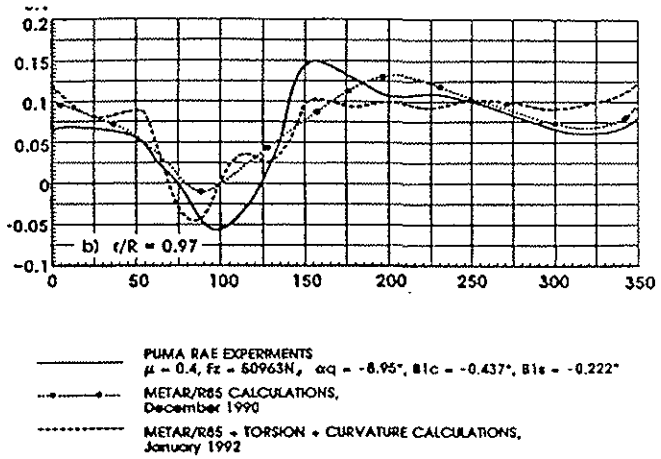

FIGURE 9 : R85 IMPROVEMENTS ON LOCAL LIFT ($C_z M^2$) CORRELATIONS

Mainly, the combination of torsion and no straight geometry in the calculation allowed to predict the negative peak of lift on the advancing side (90°), though the phase is not yet correctly predicted. Undergoing research tends to assess that an unsteady model on the lift coefficient is necessary to reproduce the lag of phase.

3.2 Validation on ROSOH (soft in torsion rotor for helicopter) experimental program

The ROSOH wind tunnel data base is aimed at allowing validations on soft rotors providing large deformations, specially in torsion. Experiments were performed in Chalais-Meudon (ONERA) on soft-in-torsion blades equipped with tabs (0°, 6°, 12°) to increase torsion deformation artificially (Ref. 4).

Advance ratio of $\mu = 0$, $\mu = 0.3$, 0.35 and 0.4 were investigated. Figure 10 shows comparative results on torsion deformation at 95 % R obtained by S.P.A. method (ONERA ref. 5), and computed by R85 using the METAR vortex lattice method to calculate the induced velocities and the simple elastic model described above (§ 2).

This correlation and the following ones, when not explicitely mentionned, correspond to the case of $\mu = 0.4$, $C_{T/\sigma} = 0.075$, tab 0°.

Note that, except for the static level (not yet explained), both experiments and calculations show a dynamic torsion deformation up to 2°75. R85 well predicts the deformation on the advancing side (0° - 180°) but still lacks of dynamic response on the retreating side. Moreover, R85 gives a lag of phase for the peak at 280°, whereas experiments record it at 240° : this is certainly due to the inflow model, currently defective in the retreating side because of its prescibed wake.

Table (1) gives correlations on the harmonic analysis of tip blade torsion deformation :

TORSION	COMPUTATION	EXPERIMENTS
STATIC	-2°01	-1°24
1/2 P-P	1°38	1°40
HARM 1	1°01	0°71
HARM 2	0°58	0°79
HARM 3	0°10	0°31
HARM 4	0°040	0°015
HARM 5	0°043	0°020

The peak-to-peak is remarkably well predicted but the analysis of the harmonic distribution confirms the fact that R85/METAR gives more weight to the 1/rev oscillation compared with the 2/rev one as it was seen on Figure 10.

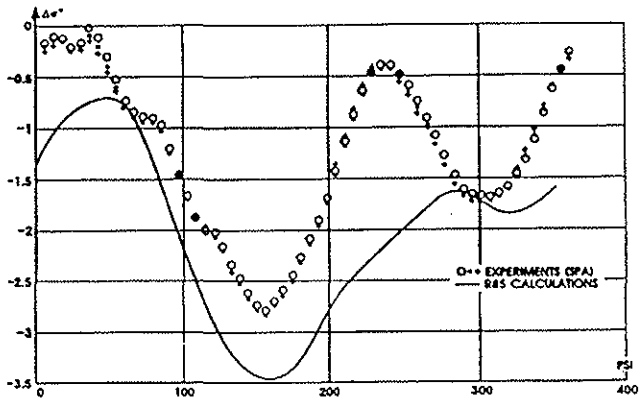

FIGURE 10 : COMPARATIVE RESULTS ON TORSION DEFORMATION : 95 % R

Figures 11, 12 and 13 show correlations on the harmonic analysis of torsion moment (Figure 11), flatwise bending moment (Figure 12) and chordwise bending moment (Figure 13). Once more, the remarkable convergence between moments calculated by force-integration and those calculated from modal curvatures is a proof of efficiency and robustness of the method described all along this paper.

Results obtained agree reasonably well with experiments, except for some high harmonics. But here, the values of strains recorded are of the level of experimental precision and those calculated of the level of computational accuracy.

To end with, a case with very large torsion deformations is computed and compared with experiments :

If, once more, the 5°5 peak to-peak-torsion deformation is well predicted, calculations amplify the 1/rev response, disregarding the 2/rev response. For such an extreme case, the lack of 2/rev in the torsion response of the code is undoubtfull.

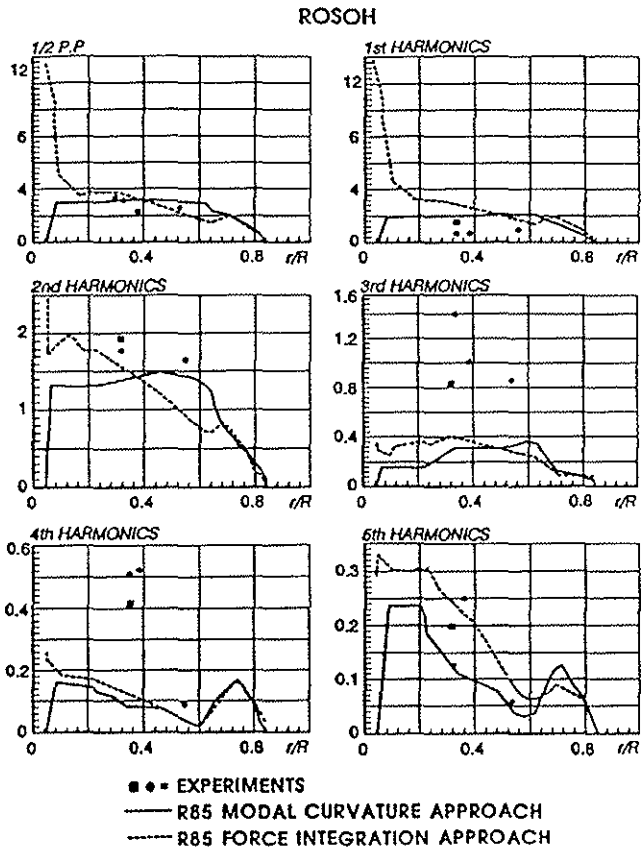

FIGURE 11 : CORRELATIONS ON THE HARMONIC ANALYSIS: TORSION MOMENT

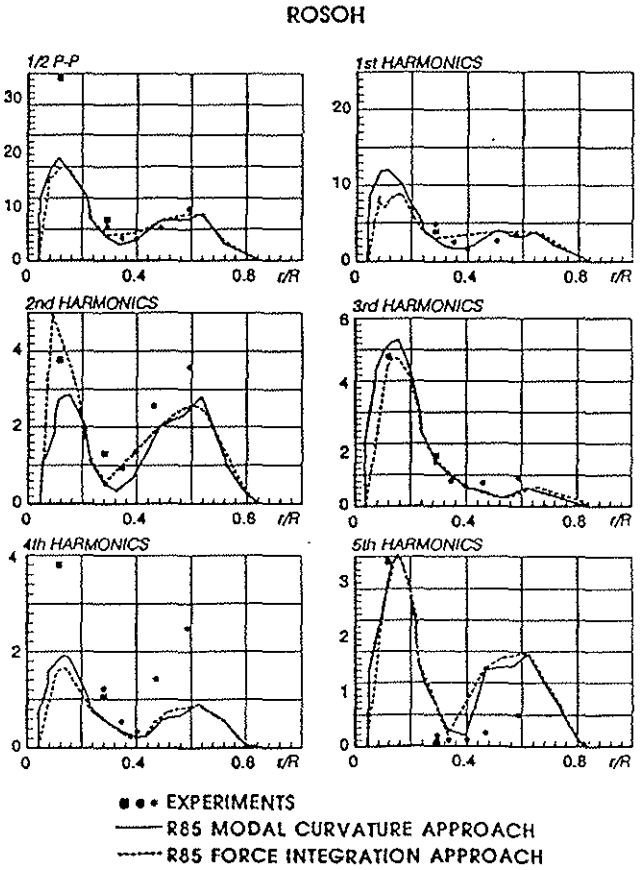

FIGURE 12 : CORRELATIONS ON THE HARMONIC ANALYSIS: FLATWISE BENDING MOMENT

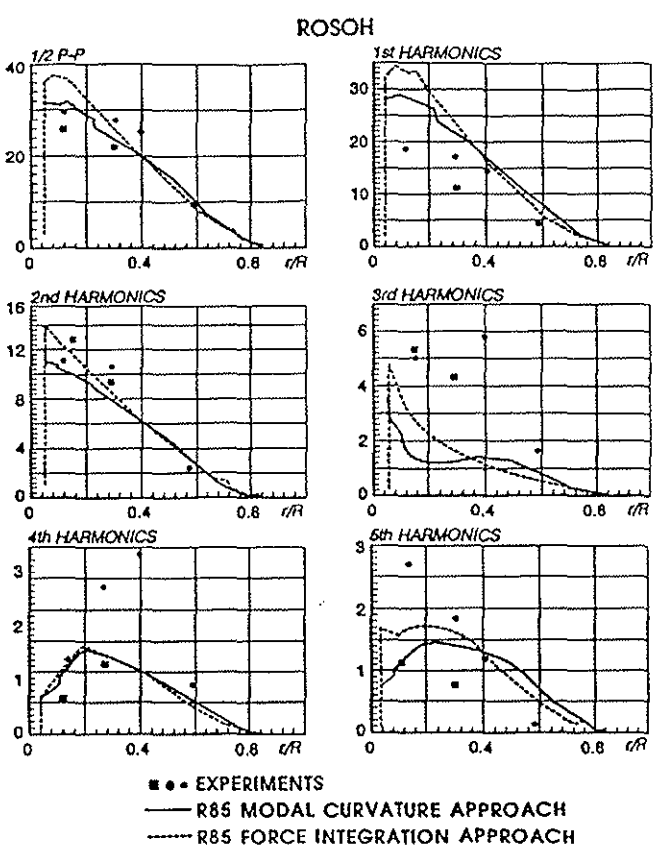

FIGURE 13 : CORRELATIONS ON THE HARMONIC ANALYSIS: CHORDWISE BENDING MOMENT

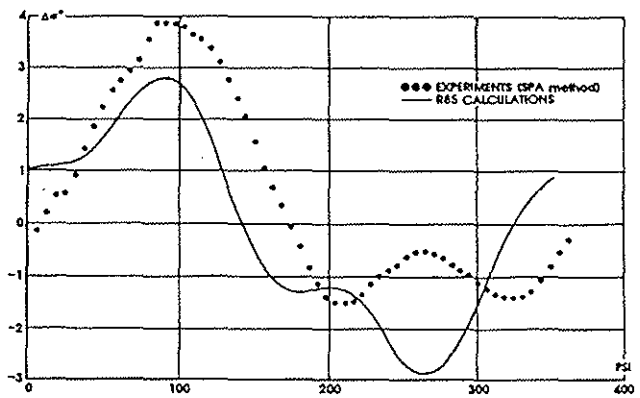

FIGURE 14 : LARGE DEFORMATION IN TORSION

4 CONCLUSION

Improvements of the soft - blade version of the R85 code allows to account for both flexion and torsion deformations. These modifications were done, keeping the modal approach for the mathematical treatment of the deformation, and the energetic approach for the resolution of the physical problem.

Validating calculations show a pretty good behaviour of the model. Effects of torsion to correlate the soft - in - torsion blade ROSOH experiments with large tip deflections have been illustrated. Improvements obtained through the PUMA RAE flight tests workshop, by combining torsion and no - straight

geometry, mainly on local parameters (C_l M^2) and moments have also been shown.

Although further improvements need to be brought in order to predict very large torsion deformations better, the R85 code is now up-to-date to develop new generations of rotors.

5 REFERENCES

(1) M. ALLONGUE, T. KRYSINSKI,
«Aéroélasticité appliquée aux rotors d'hélicoptères - Validation et application du Code R85»
27ème Colloque d'Aérodynamique Appliquée,
MARSEILLE, October 90.

(2) HOUBOLT J. C., BROOKS G. W
«Differential Equations of motion for combined flapwise bending, chordwise bending, and torsion of twisted non uniform rotor blades»,
NACA report 1346, October, 58.

(3) C. YOUNG, W. G. BOUSMAN, T. H. MAIER, F. TOULMAY, N. GILBERT,
«Lifting line prediction for a swept tip rotor blade»
AHS 47th annual forum,
PHOENIX, May 91.

(4) P. BEAUMIER, E. BERTON,
«Study of soft-in-torsion blades : ROSOH operation»
18th European Rotorcraft Forum,
AVIGNON, September 92.

(5) N. TOURJANSKY, E. SYECHENYI
«in flight blade deflection measurements by strain pattern analysis using a novel procedure»
18th European Rotorcraft Forum,
AVIGNON, September 92.